Published by :
https://www.ijert.org/
An International Peer-Reviewed Journal

International Journal of Engineering Research & Technology (IJERT)
ISSN: 2278-0181
Vol. 14, Issue 08, IESAME - 2026

Fatigue Life Estimation and Reliability Analysis Automotive Components using Finite Element and Multi-Body Dynamics

Bhuvan Athresh S Mahesh Mokshith M L, Shashikanth G S Pranesh K G, Babu K N,
Department of Mechanical Engineering
Akash Institute of Engineering and Technology
Devanahalli, Bengaluru, Karnataka, India
bhuanathresh@gmail.com, maheshm793@gmail.com, shashi063@gmail.com, praneshnihaar@gmail.com, babu.mech402@gmail.com

***Abstract*— Each component in a vehicle has infinite degrees of freedom during its working and is acted upon by various unknown forces and it's impossible to formulate and find efficiency of these components with infinite degrees of freedom. However, with the help of FEM and ADAMS It is feasible to lower degrees of freedom from infinite to finite by discretization and to extract dynamic load on each component. The precision of the solution totally depends on the inaccuracy in discretization that arises from transforming the physical system into a finite element model. In this assignment, the describes design of automobile components-based strength of material and based on the fatigue. The merits and limitations of these Furthermore, two techniques were discussed. A case study on the failure of automobile brake disc is also discussed here. Also, the various methods to improve the life of this component are also mentioned. Tells the loading cycle applied on the engine piston during the motion of the piston with velocity 24 m/s, also a simple structural and thermal examination was performed on the piston by taking peak load from the ADAMS software. However, during the analysis the justification for choosing the element size, order, type is also discussed here. Finally, the fatigue life of the piston is estimated using S-N curve. Along with this, the effect of given temperature regarding the wear and tear life of the piston is also explained in this part of the assignment. His part describes various possibilities of the crank shaft failure. And Fault tress analysis is also done to explain sequence and order of these causes by using logic gates. as demand increases for robust products with high reliability and low manufacturing and operating costs, probabilistic design techniques are being used extensively. to design reliability directly into products the purpose of this part is to demonstrate the methodology of reliability analysis based on physics of failure by using the example of fatigue failure of crankshafts. To predict life under fatigue and it also can be generalized for other failure modes.**

Keywords*— strength and fatigue, dynamic load, ADAMS software

1.INTRODUCTION

1.1 Role of fatigue consideration in automotive:

In all automotive components the Structural fatigue is very common since almost all components in automobiles are subjected to cyclic loads. Designing against fatigue becomes more challenging and process involves lots of experimental testing. Components can be designed for fatigue type of loadings. This approach leads to exact designing of parts since all the correction factors are included to endurance limit of the material. Allows parts to be designed for applications based on criteria such as damage tolerance, failure safety, unlimited life, and safe life. By using the fatigue-based approach, The automobile vehicle's endurance limit components is further reduced by considering various factors for fatigue. By this approach, the exact life of the component is got which is more reliable than other approaches. Stress life (S-N) method uses nominal stresses and relates that to local fatigue strengths for stress concentrated areas. From strain life approach, local strains from global and nominal stresses and strains can be determined.

1.2 Case study on the Failure of the Brake disc:

The disc brake in the automobile is exposed to very huge temperature stress during braking. And during this the high G-deceleration generates temperature as up to 900 degree Celsius in a fraction of a second. These high temperatures leads to thermal cracks which causes surface cracks, some macroscopic cracks and plastic deformation in the disc. When a vehicle is left unused for a long period, the discs will which is exposed to the weather get affected, the outer surface of the disc becomes rusty and pitted. This pitting caused does not leads to failure or imbalance, instead it causes severe judder when the brakes were tested in the rolling road brake tester. Most of the automotive break are constructed of cast iron, which when exposed to moisture causes corrosion immediately. However, during operation, the braking force applied on the break disc will remove any surface rust is quickly by the brake pads. But in a small sized vehicle, such breaking forces are much lower and may not clean corrosion from the surface completely, this light corrosion gets worse and leads to surface pitting which is acceptable if it does not seriously weaken the discs. Front discs will wear and become too thin. Also, because of the heating and cooling can cause the brake disc to change shape.

The slip roads are one of worst situation and this type of heavy braking is more likely to contribute to disc warping and hence break judder etc. If the brake pad friction material is allowed to wear completely then the metal backing material of the pad will run on the disc and cause scoring. a distressing metallic noise will come when the brakes are applied. This can result from a lack of servicing.

1.3 Methods to improve the life of the brake disc:

International Journal of Engineering Research & Technology (IJERT)
ISSN: 2278-0181
Vol. 14, Issue 08, IESAME - 2026

The use of surface compressive stressing to increase fatigue life is based on two facts; fatigue is a surface phenomenon and fatigue is a tension effect (Henry n. d.). Based on this several techniques like Cold Local Yielding (overloading, straightening and cold forming, peening tumbling, and surface rolling), Hot Local Yielding (quenching, flame cutting, welding, and grinding) and Transformation (quench hardening, carburizing and nitriding) are being used to improve the fatigue life depending upon the application and manufacturing process (Henry n. d.). For rear axle shot peening, induction hardening, quenching and shot blasting are more commonly used the procedure of shot peening involves cold working. to creates a layer of compressive residual tension. This process entails impacting a surface containing bits of glass, ceramic, or metal splattered around with enough force to induce distortion of plasticity. This plastic deformation creates internal tensile tension and residual compressive stress in a peened surface. Surface compressive stress resists metal fatigue (Latem 2014). The initiation site for fatigue failure in rear axles occurs usually in splines, keyways, or the major change in cross section where the major diameter of the shaft meets the flange. In a case study of automotive rear axles discovered that shot peening of the rear axle increased the fatigue strength from 13,000 psi to 43,000 psi (Kenneth 1985). Induction process It is through hardening that an axle shaft is passed through an electrical coil in which it is heated to red hot and then quenched to make it hard. It is estimated that 25 – 30 % of fatigue strength is increased to the axles by this hardening process (Dutchman 2014). Shot blasting concentrates abrasive particles at high speed of 65-110 m/s in a controlled manner at the component thereby removing surface contaminates. Small steel balls and granules of silicon carbide are most used abrasive particles to enhance fatigue life (Corrosionpedia2014). In a study on shot blasting process by General Motors it was found that using this process on automotive axles a 56 % increase on fatigue life was achieved (Almen 1943).

The prevention and improving life of the automotive from fatigue failure are listed out here:

- Regularly go for wiggling of the brake pad, calipers, and other brake related components.
- Look for the loosen parts of the break and tighten it frequently to prevent vibrate and noise.
- Look for the worn out components of the disc and install new.
- Replacement is done with same material and size, also check manual and configuration of the material for proper servicing.
- Brake fluid is the most important component which must be replaced after each mentioned kilometers in the user manual.
- In case the pads are in good condition and still having problem then it's the time to check brake pad gasket. Any problem in the gasket leads to brake squeal.
- Also, the failure in the brake disc will alter steering wheel alignment. Due to this misalignment the vehicle may pull to one side during braking. Thus, the inspection of brake rooter is also must.

2. METHODOLOGY AND SCOPE OF PRESENT INVESTIGATION

The study starts by selecting a structural component that experiences cyclic or fluctuating loads during its service life. Material data, including fatigue strength, Young's modulus, and fracture toughness, are gathered from standards or experimental sources. Loading conditions are identified through operational data or simulations, including amplitude and frequency of loads. Finite Element Analysis (FEA) is used to model the component and determine stress and strain distributions under loading. Fatigue life is estimated using stress-life (S-N) or strain-life (ε-N) methods based on the nature of the material and load cycles. The cumulative damage is calculated using Miner's Rule to assess the total life under variable amplitude loading. Crack initiation and growth are modelled using fracture mechanics, such as Paris' Law, to predict structural failure. Probabilistic models are introduced to account for uncertainties in loading, material properties, and manufacturing tolerances. A reliability analysis is performed to calculate the probability of failure over the structure's intended lifespan. Monté Carlo simulation is used to assess the impacts of random variations and assess overall structural reliability. Using sensitivity analysis, one may ascertain which input parameters most influence fatigue life and reliability. Results indicate that small deviations in load or material behavior can drastically reduce fatigue life. High-stress regions identified in the FEA correspond well with typical failure locations seen in physical components. The discussion reveals that ignoring variability can lead to overestimated safety margins or unexpected failures. Reliability indices derived from the analysis offer quantitative insights into structural safety levels. Design changes, such as improving geometry or using higher fatigue-resistant materials, are suggested for improved life. Maintenance planning is optimized based on predicted fatigue life and probability of failure thresholds. The study highlights the importance of integrating fatigue and reliability analysis into early design stages.

3. EXPERIMENTAL METHODS

3.1 Dynamic analysis using MSC. ADAMS:

Creo parametric is an excellent 3D modeling software and is ideal for capturing the design intent of the any physical model. The the geometric models of the single cylinder engine created in Creo software.

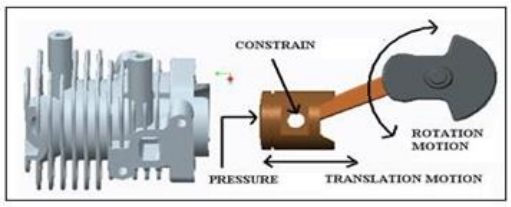

Figure 3.1.1 Geometric model of Engine created using Creo software.

Engine mechanism is the mostly used mechanism in any automotive applications. A multi-body system dynamics model based on ADAMS software is built to carry out virtual experiments. To apply pressure load on the piston the inertial loads of the piston were calculated as loading cycles byusing Adams software. Here, all the engine components are included with required constraints and material properties (Figure 3.1.3)

International Journal of Engineering Research & Technology (IJERT)
ISSN: 2278-0181
Vol. 14, Issue 08, IESAME - 2026

and the piston is made to translate at velocity of 24 m/sec as given by the module leader.

In this mechanism total 5 links are present including a ground link and a sliding link. Figure 3.1.3 shows the different joints defined for the engine model in which the revolute joint specified in the crank was given a motion of 33,200 deg/sec for the piston to reach a velocity of 24 m/s.

The below figure 3.1.3 shows the simulation piston cylinder in ADAMS along with piston velocity and loading cycle curves.

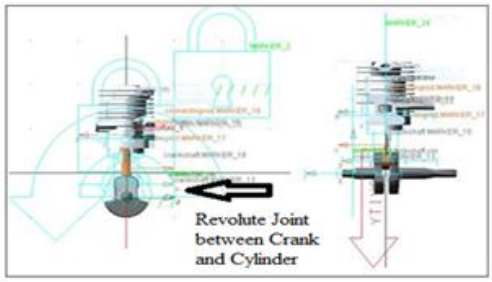

Figure 3.1.2 multi-body system dynamics model of engine based on ADAMS software.

The piston velocity graph in which the maximum piston velocity is 24 m/s is shown below.

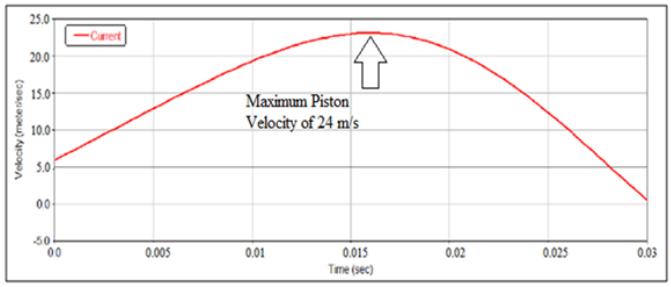

Figure 3.1.3 Piston velocity curve obtained in ADAMS Software.

The maximum inertial force of the engine measured from the Adams analysis at 24 m/s is 756 N.

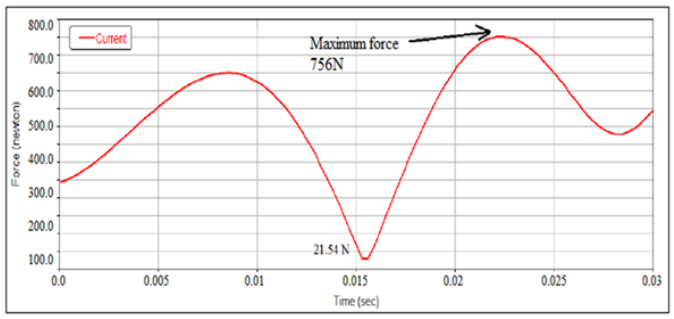

Figure 3.1.4 Inertia force vs time plot.

The total pressure on the piston is calculated as shown below. The gas pressure acting on a 4 inch diameter piston in Spark Ignition engines will be around 10 MPa, whereas in CI engines will be around 20 MPa.

For the 100 mm diameter CI engine piston the gas force is taken as 96000 N.

Total Force acting on the Piston F = Gas Force – Inertia Force

= 96000 – 756.

F = 95244N

Total Pressure acting on the Piston P	=	Total Force acting on the Piston / Piston Area
	=	95,244 / (π/4)* D2
P	=	12.1268 MPa

Thus the pressure applied on the crown surface is 12.1268 MPa.

3.2 Structural analysis of piston:

The given engine piston is converted in to a finite FEA model through discretization by second order tetrahedral mesh. The finite element model of the piston provided with rigid elements at the two piston pin holes along with displacement constraints applied at the master node.

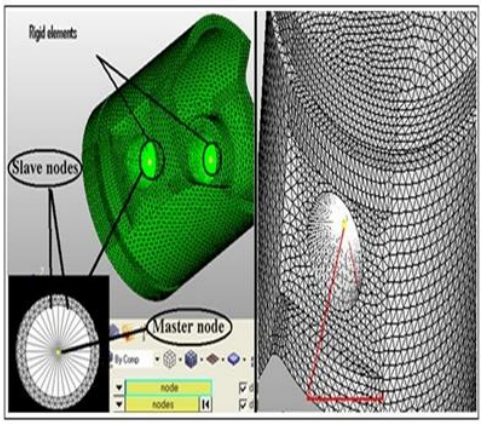

Figure 3.2.1 Piston with rigid elements and displacement constraints applied at master nodes.

Properties:

Name:	AISI Type A2 Tool Steel
Model type:	Linear Elastic Isotropic
Default failure criterion:	Max von Mises Stress
Density ρ	7860 kg/m3,
Young's Modulus E	205 GPa
Poisson's ratio υ	0.3

The following Figure shows the boundary conditions used for structural analysis of piston.

Loads and Fixtures:

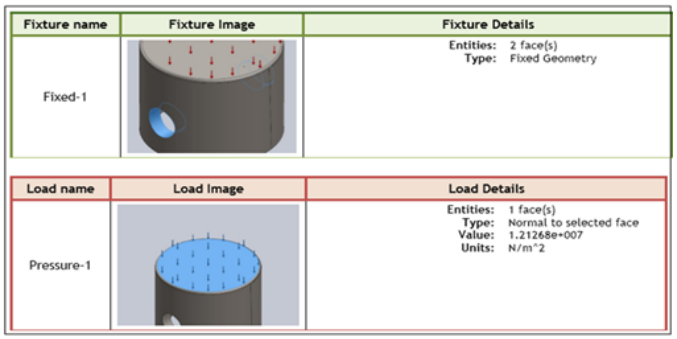

Figure 3.2.2 Boundary conditions applied on the piston.

Grid independence study:

Case 1: Coarse mesh

Mesh type	Solid Mesh
Jacobian points	4 Points

International Journal of Engineering Research & Technology (IJERT)
ISSN: 2278-0181
Vol. 14, Issue 08, IESAME - 2026

Element Size	0.0126846 m
Total Nodes	2437
Total Elements	1163
Maximum Aspect Ratio	5.7329
% of elements with Aspect Ratio < 3	92.1
% of elements with Aspect Ratio > 10	0
% of distorted elements(Jacobian)	0
Time to complete mesh(hh;mm;ss):	00:00:06

Table 3.1 Mesh information.

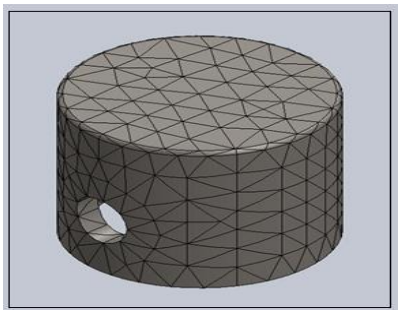

Figure 3.2.3 Piston with course Mesh.

Study Results:

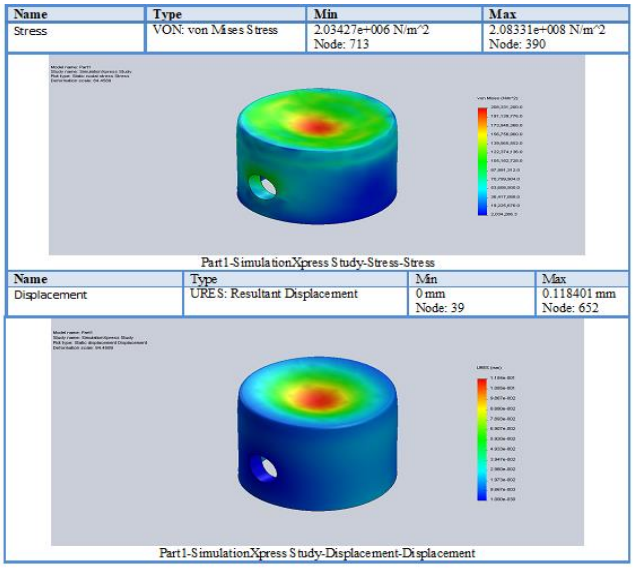

Figure 3.2.4 Von-mises stress and displacement plot.

Case 2: Medium mesh size:

Mesh type	Solid Mesh
Jacobian points	4 Points
Element Size	0.00665941 m
Total Nodes	0.000332971 m
Total Elements	12269
Maximum Aspect Ratio	7064
% of elements with Aspect Ratio < 3	4.4043
% of elements with Aspect Ratio > 10	99.5
% of distorted elements(Jacobian)	0
Time to complete mesh(hh;mm;ss):	0

Table 3.2 Mesh information.

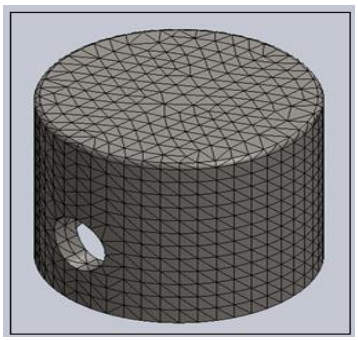

Figure 3.2.5 Piston with medium mesh size.

Study Results:

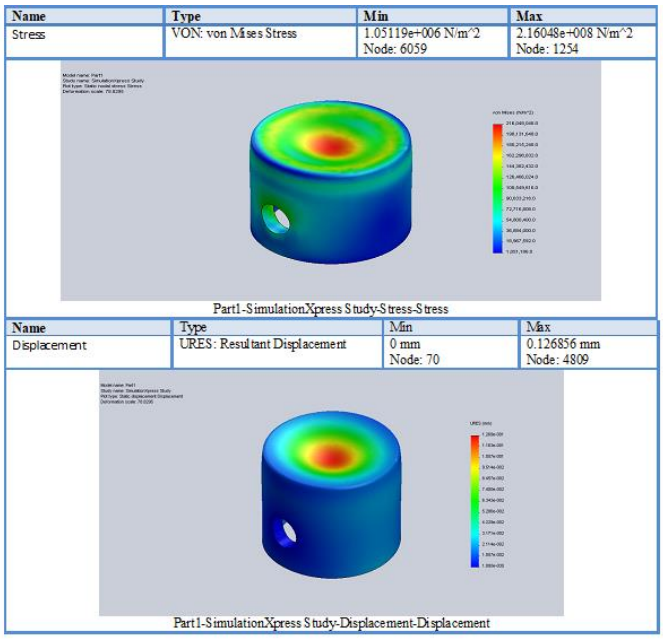

Figure 3.2.6 Von-mises stress and displacement plot.

Case 3: Fine mesh size:

Mesh type	Solid Mesh
Jacobian points	4 Points
Element Size	0.00317115 m
Total Nodes	78424
Total Elements	50047
Maximum Aspect Ratio	4.0932
% of elements with Aspect Ratio < 3	99.9
% of elements with Aspect Ratio > 10	0
% of distorted elements(Jacobian)	0
Time to complete mesh(hh;mm;ss):	00:00:42

Table 3.3 Mesh information.

International Journal of Engineering Research & Technology (IJERT)
ISSN: 2278-0181
Vol. 14, Issue 08, IESAME - 2026

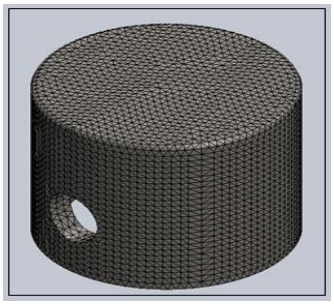

Figure 3.2.7 Piston with fine mesh size.

Study Results:

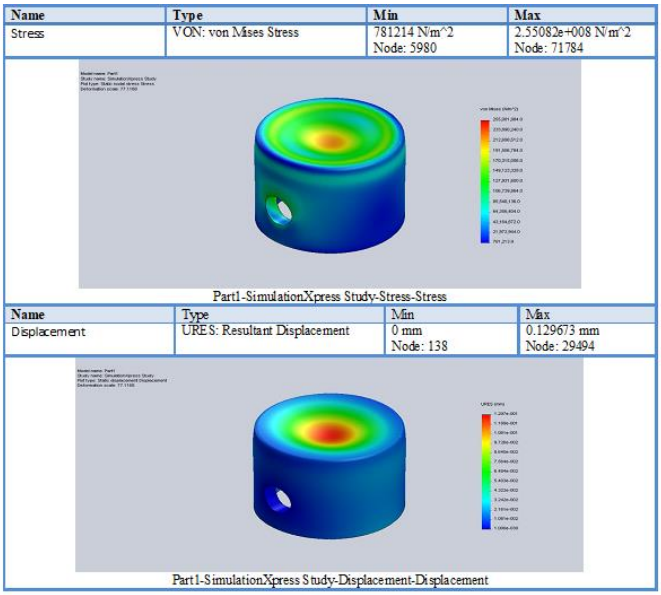

Figure 3.2.10 Von mises stress and displacement plot.

Maximum stress of 255 MPa is created on the inner edge of the piston due to high tensile bending stress creation. It is because it is the region which is subjected to more loads exerted by the gas force and inertia force. The yield strength of piston is 395 MPa for the selected material is well above the produced stress thus the piston will not fail.

4 RESULTS AND DISCUSSIONS

Fatigue life estimation with suitable correction factor:

Correction Factors for the Piston

Surface factor:

The piston is machined since most of the steel pistons are casted and then machined to get smooth surface.

Ka = A (σu) b where, A = 4.51; b = - 0.265 and Ultimate Strength σu = 655 MPa.

Ka = 4.51 (655) - 0.265

Ka = 0.809

Loading factor:

Piston is subjected to bending

For axial loading Kc = 1 [13].

Stress concentration factor:

Kf = 1 + q (kt -1) where, d / D = 25 / 100 = 0.25; notch radius r = 2.5 mm q is the notch

sensitivity factor = 0.85; kt is the stress concentration factor = 1.95

Kf = 1.808

Size Modification Factor:

The piston is subjected to bending

Kb = 1.24 (d)-0.107 where, d is 25 mm (Gudgeon pin hole)

Kb = 0.879

Temperature Modification Factor:

The maximum operating temperature is 500° C

So the temperature modification factor Kd = 0.768.

Fatigue Stress Concentration Factor:

Kf = 1 + q (kt -1) where, d / D = 25 / 100 = 0.25; notch radius r = 2.5 mm q is the notch

Sensitivity factor = 0.85; kt is the stress concentration factor = 1.95

Kf = 1.808

Calculation of S-N Curve:

<u>Without temperature factor</u>

Endurance Limit (Uncorrected)

σe' = f2 σu

σe' = 0.5 655

σe' = 327.5 MPa

Endurance Limit (Corrected)

σe = (Ka Kb Kc σe') / Kf

= (0.809 0.879 1 327.5) / 1.808

σe = 128.81 MPa

Fatigue Strength Coefficient

$$a = \frac{(f1 \times \sigma u)^2}{\sigma e}$$

a = 2697.85 MPa

Fatigue Strength Exponent

$$b = \frac{\log\left(\frac{f1 \times \sigma u}{\sigma e}\right)}{\log\left(\frac{N_1}{N_2}\right)}$$

b = - 0.165

Stress at 10^3 cycles

σ1 = f1 * σu = 0.9 * 655

International Journal of Engineering Research & Technology (IJERT)
ISSN: 2278-0181
Vol. 14, Issue 08, IESAME - 2026

σ1 = 589.5 MPa

Stress at 10^4 cycles

σ2 = a (N)^b = 2697.85 (10^4)^- 0.165

σ2 = 590.225MPa

Corrected value σ2 = 496.581 MPa

Stress at 10^5 cycles

σ3 = a (N)^b = 2697.85 (10^5)^- 0.165

σ3 = 403.662 MPa

Stress at 10^6 cycles

σ4 = a (N)^b = 2697.85 (10^6)^- 0.165

σ4 = 276.069 MPa

Stress at 10^7 cycles

σ5 = σe = 128.81 MPa

With temperature factor

Endurance Limit (Uncorrected)

σe' = f2 σu

σe' = 0.5 655

σe' = 327.5 MPa

Endurance Limit (Corrected)

σe = (Ka*Kb*Kc*Kd*σe') / Kf

= (0.809*0.879*1*0.768*327.5) / 1.808

σe = 98.93 MPa

Fatigue Strength Coefficient

$$a = \frac{(f1 \times \sigma u)^2}{\sigma e}$$

a = 3512.83 MPa

Fatigue Strength Exponent

$$b = \frac{\log\left(\frac{f1 \times \sigma u}{\sigma e}\right)}{\log\left(\frac{N_1}{N_2}\right)}$$

b = - 0.194

Stress at 10^3 cycles

σ1 = f1*σu = 0.9*655

σ1 = 589.5 MPa

Stress at 10^4 cycles

σ2 = a (N)^b = 3512.83 (104)- 0.194

σ2 = 588.379 MPa

Corrected value σ2 = 482.953 MPa

Stress at 10^5 cycles

σ3 = a (N)^b = 3512.83 (105)- 0.194

σ3 = 376.406MPa

Stress at 10^6 cycles

σ4 = a (N)^b = 3512.83 (106)- 0.194

σ4 = 240.8 MPa

Stress at 10^7 cycles

σ5 = σe = 98.93 MPa

S-N curve:

Without temperature factor

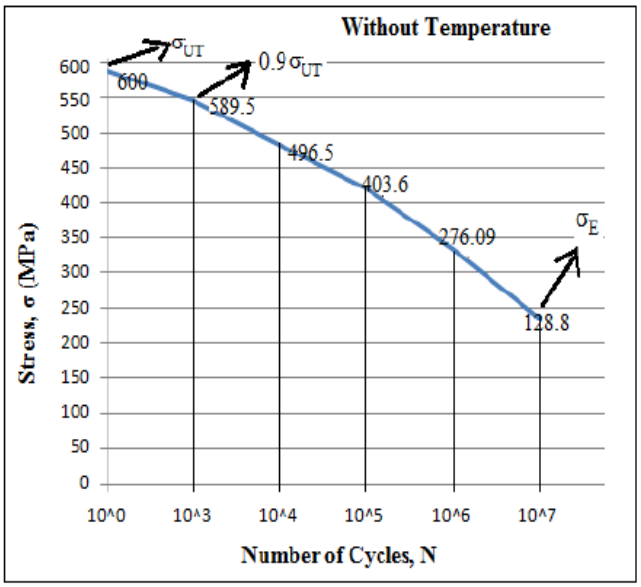

Figure: 4.1 S-N Curve without Temperature factor

With temperature factor

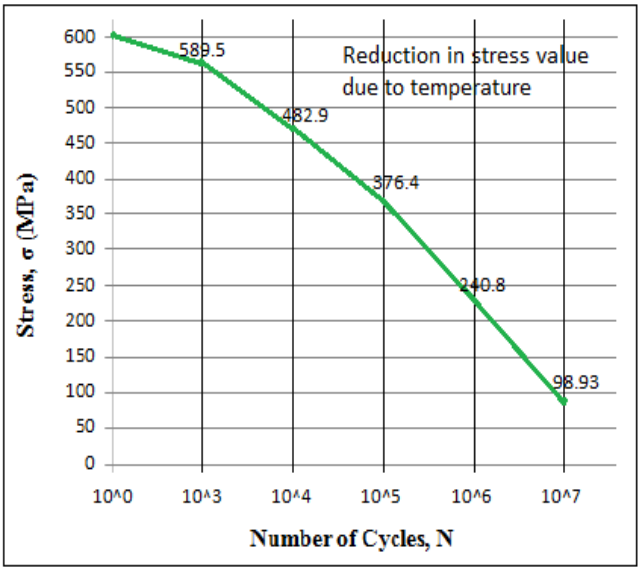

Figure: 4.2 S-N Curve with Temperature factor

International Journal of Engineering Research & Technology (IJERT)
ISSN: 2278-0181
Vol. 14, Issue 08, IESAME - 2026

Due to raise in the temperature, the piston is subjected to more fatigue load which fails at even less working stress compared to the stress at room temperature. It is also absorbed that when the temperature is raised, the working stress is reduced even more and fails at a faster rate than the intended working requirements.

Fatigue Life Estimation of Piston without Temperature Factor:

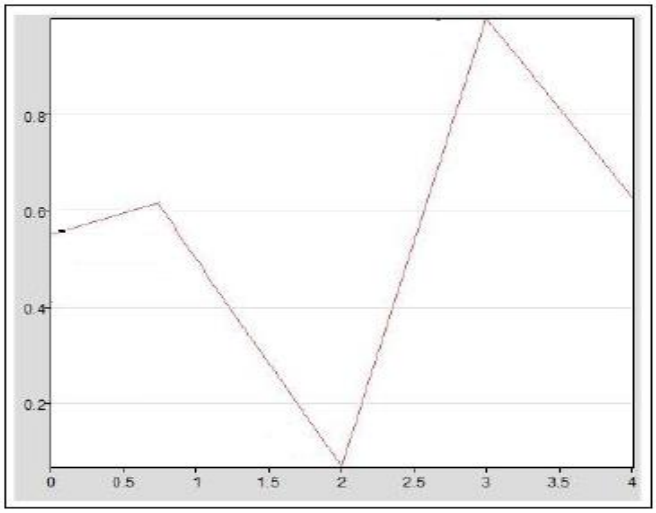

Figure: 4.3 Cyclic Loading Pattern

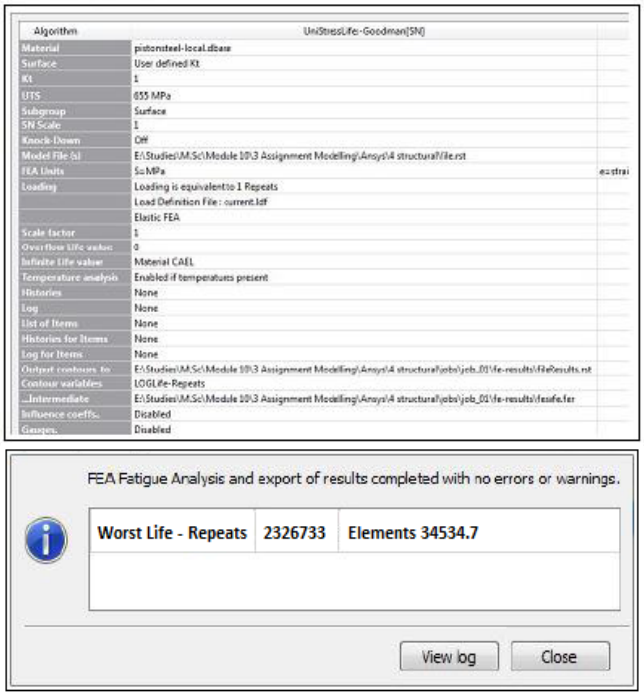

Figure: 4.4 Fatigue life Estimation without Temperature Factor

Worst life of 2.3 x 10^6

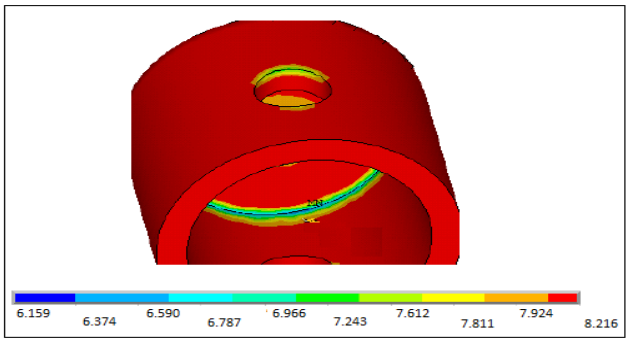

Figure: 4.5 FE Cycle of the Piston

Maximum life cycle of the piston is 8.216.

The minimum life cycle is 6.159.

Fatigue life = N = 10((log (σ/ a) / b)

= 10^6.159.

Fatigue Life with temperature factor included:

k = 93.9 Wm^-1.k^-1

Temperature boundary condition = 773 K

Heat transfer coefficient = 2724 W/m2.K

Bulk temperature of 303 K (30°C).

Heat transmission as a convection boundary condition

Coefficient = 91 W/m2.K and

Bulk temperature of 303 K (30°C)

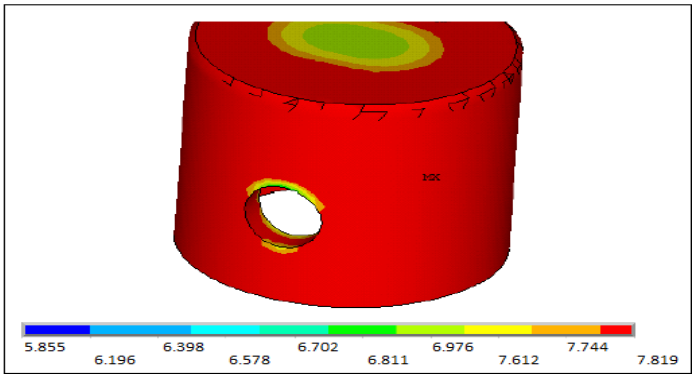

Figure: 4.6 FE life with Temperature factor

Fatigue life = N = 10((log (σ/ a) / b) = 10^5.855.

Crank shafts may fail for a variety of reasons and some commonly noticed reasons which causes the crank shaft to fail are manufacturing defects, improper loading cycle, in sufficient lubrication, sensor malfunctioning or no proper servicing of the vehicle etc. hence, understanding of these issues are very important in order to prevent failure and to enhance the life of the automobile components.

CONCLUSIONS

This thesis successfully demonstrates an integrated simulation-driven methodology for the fatigue life and reliability assessment of critical automotive components. The research establishes a robust workflow, transitioning from dynamic load extraction in MSC ADAMS to detailed structural and thermal Finite Element Analysis (FEA) in ANSYS, and

International Journal of Engineering Research & Technology (IJERT)
ISSN: 2278-0181
Vol. 14, Issue 08, IESAME - 2026

finally to fatigue life estimation using the stress-life (S-N) approach.

A pivotal finding of this investigation is the profound and quantifiable impact of elevated temperature on component durability. The analysis revealed that the endurance limit of the AISI Type A2 steel piston dropped significantly from 128.81 MPa at room temperature to 98.93 MPa at an operating temperature of 500°C. This reduction precipitated a substantial decrease in predicted fatigue life, underscoring the critical necessity of incorporating thermal effects for accurate life prediction. The study further validated the piston's structural integrity under peak static loading, with a maximum von Mises stress of 255 MPa remaining below the material's yield strength.

Complementing the piston analysis, a systematic Fault Tree Analysis (FTA) of crankshaft failure provided a structured framework for understanding complex failure causality, paving the way for probabilistic reliability analysis. In summary, this work conclusively shows that a holistic approach—integrating multi-body dynamics, FEA, and fatigue analysis while accounting for real-world operational factors like temperature—is essential for designing safer, more reliable, and longer-lasting automotive components, moving beyond the limitations of traditional deterministic methods.

REFRERENCES

[1] Tokaji, K. 2006. High Cycle Fatigue Behavior of Ti-6Al-4V Alloy at Elevated Temperatures. Scripta Materialia. 54: 2143–2148.
[2] Zhu, X., Shyam, A., Jones, J. W., Mayer, H., Lasecki, J. V., Allison, J. E. 2006. Effects of Microstructure and Temperature on Fatigue Behavior of E319-T7 Cast Aluminum Alloy in Very Long-Life Cycles. International Journal of Fatigue. 28: 1566–1571.
[3] Pereira, H. F. S. G., de Jesus, A. M. P., Ribeiro, A. S., Fernandas, A. A. 2008. Influences of Loading Sequence and Stress Ratio on Fatigue Damage Accumulation of a Structural Component. Science and Technology of Materials. 20: 60–67.
[4] Liu, Y., Yu, J. J., Xu, Y., Sun, X. F., Guan, H. R., Hu, G. Q. 2007. High Cycle Fatigue Behavior of a Single Crystal Super Alloy at Elevated Temperatures. Materials Science and Engineering A. 454–455: 357–366.
[5] Uematsu, Y., Akita, M., Nakajima, M., Tokaji, K. 2007. Effect of Temperature on High Cycle Fatigue Behavior in 18Cr-2Mo Ferritic Stainless Steel. International Journal of Fatigue. 30: 642–648.
[6] Jiujerm, P., ltenberger, I.A. 2007. Effect of Temperature on Cyclic Deformation Behavior and Residual Stress Relaxation of Deep Rolled Under-aged Aluminum Alloy AA6110. Materials Science and Engineering A. 452–453: 475–482.
[7] Kolios, A., Shittu, A. A., and Mehmanparast, A. (2020). a thorough examination of structural reliability techniques for offshore jacket structure fatigue and deformation study. Metals, 11(1), 50.
[8] Bignonnet, A., Gayton, N., and Echard, B. (2014). An approach to fatigue design reliability analysis. Journal of Fatigue International, 59, 292-300.
[9] In January of 2023, Xu, C., Lei, H., and Wang, G. Based on long-term health monitoring data, fatigue life and fatigue reliability are evaluated for long-span spatial structures. pp. 586–594 in Structures, vol. 47. Elsevier.
[10] Sobczykiewicz, W., Jakubczak, H., and Glinka, G. (2006). robustness of structural elements under fatigue. Journal of Materials and Product Technology International, 25(1-3), 64-83.